J|A|C|S ARTICLES

Published on Web 06/18/2010

Arrested Catalysis: Controlling Kumada Coupling Activity via a Redox-Active N-Heterocyclic Carbene

Andrew G. Tennyson, Vincent M. Lynch, and Christopher W. Bielawski*

Department of Chemistry and Biochemistry, The University of Texas at Austin, 1 University Station A5300, Austin, Texas 78712

Received April 7, 2010; E-mail: bielawski@cm.utexas.edu

Abstract: Optimized syntheses for 1,3-dimesitylnaphthoquinimidazolium chloride [**1**H][Cl] and the corresponding silver−NHC complex [AgCl(**1**)] (**2**) were developed, enabling access to this versatile reagent in near-quantitative yield. Transmetalation from **2** to $[NiCl_2(PPh_3)_2]$, *trans*-$[PdCl_2(PhCN)_2]$, or *trans*-$[PtCl_2(PhCN)_2]$ afforded the Group 10 complexes *trans*-$[MCl_2(\mathbf{1})_2]$ (**3a**−**c**, M = Ni, Pd, and Pt, respectively) in excellent overall yield (>95%) after three steps from commercially available starting materials. Electrochemical measurements indicated that the $E_{1/2}$ and $\Delta E_{1/2}$ values for the quinone reduction couples were independent of the identity of the bridging transition metal in these complexes. Whereas attempts to isolate the reduced complexes were unsuccessful, UV/vis spectroelectrochemical analysis confirmed that electrochemical reduction of **3a**−**c** in situ afforded optical difference spectra consistent with the formation of the expected reduced species. Complex **3a** was found to catalyze the Kumada cross-coupling reaction between PhMgCl and a range of bromoarenes at room temperature. Addition of 2 equiv of cobaltocene (with respect to **3a**) to the coupling reaction with bromotoluene caused a decrease in catalytic activity (from 4.7×10^{-5} to 2.7×10^{-6} s^{-1}), which was attributed to the conversion of **3a** to an arrested state. Subsequent introduction of ferrocenium tetrafluoroborate (2 equiv with respect to **3a**) restored a significant degree of catalytic activity ($k_{obs} = 1.2 \times 10^{-5}$ s^{-1}). Redox-switching experiments performed over different time scales revealed that the catalyst was stable in the reduced/inactive state and that extended durations in this state did not impede catalytic reactivation upon subsequent oxidation.

Introduction

N-Heterocyclic carbenes (NHCs) were originally proposed by Breslow as intermediates in the hydrogen−deuterium exchange of thiazolium salts over a half-century ago.[1] Shortly thereafter, Wanzlick demonstrated that these molecules can exist in equilibrium between free carbenes and tetraazafulvenes or other dimeric derivatives,[2] the latter of which were shown to enable access to complexes of NHCs with various metals[3] and electrophiles.[4] Nonetheless, it was not until the preparation and isolation of the first crystalline carbene by Arduengo[5] in 1991 that NHCs began to receive widespread attention. Since then, NHCs have become prevalent in many disciplines, including the coordination chemistry[6] of transition metals,[7] lanthanides,[8] and main group elements,[9] organic[10,11] and organometallic[12,13] catalysts, polymers,[14] antibiotics,[15] and optoelectronics.[16]

Perhaps the most visible impact of NHCs has been their near-ubiquitous use in supporting transition metal-based catalysts, given that their coordination chemistry is similar to that of phosphines,[17,18] yet their complexes are more resistant to ligand displacement due to their greater σ-donicity.[19,20] In addition,

(1) Breslow, R. *J. Am. Chem. Soc.* **1957**, *79*, 1762–1763.
(2) Wanzlick, H. W.; Esser, F.; Kleiner, H. J. *Chem. Ber.* **1963**, *96*, 1208–1212.
(3) Öfele, K. *J. Organomet. Chem.* **1968**, *12*, P42–P43.
(4) Winberg, H. E.; Coffman, D. D. *J. Am. Chem. Soc.* **1965**, *87*, 2776–2777.
(5) Arduengo, A. J., III; Harlow, R. L.; Kline, M. *J. Am. Chem. Soc.* **1991**, *113*, 361–363.
(6) Hahn, F. E.; Jahnke, M. C. *Angew. Chem., Int. Ed.* **2008**, *47*, 3122–3172.
(7) Lin, J. C. Y.; Huang, R. T. W.; Lee, C. S.; Bhattacharyya, A.; Hwang, W. S.; Lin, I. J. B. *Chem. Rev.* **2009**, *109*, 3561–3598.
(8) Arnold, P. L.; Casely, I. *J. Chem. Rev.* **2009**, *109*, 3599–3611.
(9) (a) Wolf, R.; Uhl, W. *Angew. Chem., Int. Ed.* **2009**, *48*, 6774–6776. (b) Scheschkewitz, D. *Angew. Chem., Int. Ed.* **2008**, *47*, 1995–1997.
(10) (a) He, M.; Bode, J. W. *J. Am. Chem. Soc.* **2008**, *131*, 418–419. (b) Phillips, E. M.; Wadamoto, M.; Chan, A.; Scheidt, K. A. *Angew. Chem. Int. Ed.* **2007**, *46*, 3107–3110. (c) de Alaniz, J. R.; Rovis, T. *J. Am. Chem. Soc.* **2005**, *127*, 6284–6289.
(11) (a) Kamber, N. E.; Jeong, W.; Waymouth, R. M.; Pratt, R. C.; Lohmeijer, B. G. G.; Hedrick, J. L. *Chem. Rev.* **2007**, *107*, 5813–5840. (b) Enders, D.; Niemeier, O.; Henseler, A. *Chem. Rev.* **2007**, *107*, 5606–5655.
(12) Díez-González, S.; Marion, N.; Nolan, S. P. *Chem. Rev.* **2009**, *109*, 3612–3676.
(13) Sommer, W. J.; Weck, M. *Coord. Chem. Rev.* **2007**, *251*, 860–873.
(14) (a) Boydston, A. J.; Williams, K. A.; Bielawski, C. W. *J. Am. Chem. Soc.* **2005**, *127*, 12496–12497. (b) Coady, D. J.; Khramov, D. M.; Norris, B. C.; Tennyson, A. G.; Bielawski, C. W. *Angew. Chem. Int. Ed.* **2009**, 5187–5190. (c) Norris, B. C.; Bielawski, C. W. *Macromolecules* **2010**, *43*, 3591–3593.
(15) Kascatan-Nebioglu, A.; Panzner, M. J.; Tessier, C. A.; Cannon, C. L.; Youngs, W. J. *Coord. Chem. Rev.* **2007**, *251*, 884–895.
(16) Chi, Y.; Chou, P.-T. *Chem. Soc. Rev.* **2010**, *39*, 638–655.
(17) Peris, E.; Crabtree, R. H. *Coord. Chem. Rev.* **2004**, *248*, 2239–2246.
(18) Herrmann, W. A.; Mihalios, D.; Ofele, K.; Kiprof, P.; Belmedjahed, F. *Chem. Ber. Recl.* **1992**, *125*, 1795–1799.
(19) Scott, N. M.; Clavier, H.; Mahjoor, P.; Stevens, E. D.; Nolan, S. P. *Organometallics* **2008**, *27*, 3181–3186.
(20) Jafarpour, L.; Stevens, E. D.; Nolan, S. P. *J. Organomet. Chem.* **2000**, *606*, 49–54.

10.1021/ja102686u

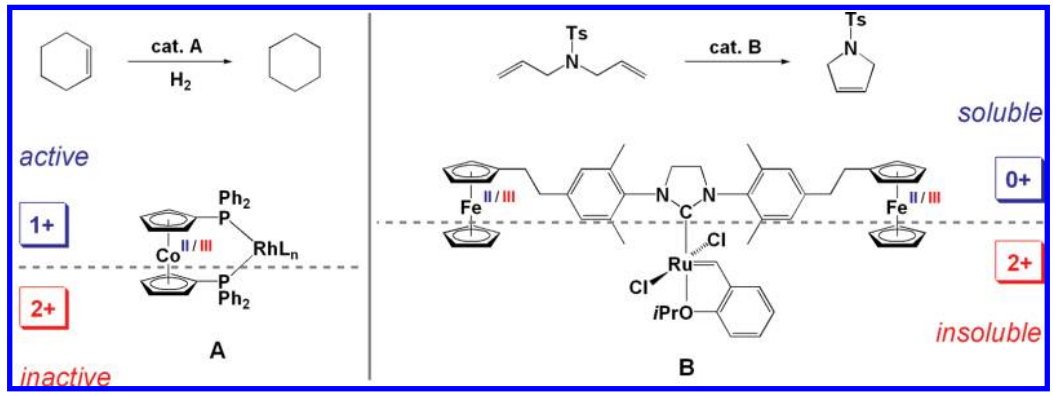

Figure 1. Examples of RSC utilizing non-NHC and NHC-supported catalysts. In their reduced states, **A** (1+) and **B** (0+) catalyze hydrogenation and ring-closing metathesis reactions, respectively (top). Upon oxidation, complex **A** (1+ → 2+) is inactivated and complex **B** (0+ → 2+) is precipitated (bottom).

many NHCs are derived from easily accessible precursors[21] and readily form organometallic complexes via the direct metallation of free NHCs[22] or transmetalation from Ag−NHC intermediates.[23] Organometallic complexes supported by NHCs enable a broad scope of reactivity, ranging from organic transformations,[24−27] such as [5+2] cycloadditions[28] and hydroformylations,[29] to polymerizations.[30] As the cost and complexity of chemical synthesis increase, however, so does the need for more efficient and atom-economic variations of these processes. Recently, tandem catalyses have shown considerable potential for merging several useful transformations into a single step by effecting multiple reactions in the same pot.[31−43] These systems typically utilize multiple catalytically active species that facilitate non-interfering, orthogonal reactions, usually in series.

An alternative approach is to employ only one catalytic species and modulate its reactivity using stimuli such as pH,[44,45] light,[46,47] and redox state changes.[48−55] Owing to the redox-active nature intrinsic to many transition metal complexes, an appealing strategy is that of redox-switchable catalysis (RSC). Seminal work by Wrighton demonstrated the ability to control the electron density, and thus reactivity, of ligated metals via oxidation state changes[56] and how these redox events could be used to modulate catalytic activity.[57] For example, complex **A** catalyzes the transfer hydrogenation of cyclohexene to cyclohexane when the cobaltocene moiety is in a neutral state (Figure 1A, top). However, oxidation from Co^{II} to Co^{III} affords a less-donating cobaltocenium-based ligand and is accompanied by a loss in catalytic activity (Figure 1A, bottom). More recently, Gibson and Long utilized a similar strategy to prepare a lactide polymerization catalyst that could be deactivated and reactivated upon chemical oxidation and reduction, respectively.[51] Around the same time, Plenio demonstrated that incorporating ferrocene groups within a Grubbs-type catalyst (complex **B**, Figure 1B top) can facilitate recovery, where oxidation causes the catalyst to precipitate from the reaction solution, enabling simple physical separation via filtration (Figure 1B bottom).[52] Despite the success of these strategies, we have found no reports of RSC that employ Group 10 complexes or NHC-type ligands with redox-active groups integrated into their architecture.

(21) Peris, E. *Top. Organomet. Chem.* **2007**, *21*, 83–116.
(22) Herrmann, W. A.; Köcher, K. *Angew. Chem., Int. Ed.* **1997**, *36*, 2163–2187.
(23) Wang, H. M. J.; Lin, I. J. B. *Organometallics* **1998**, *17*, 972–975.
(24) Díez-González, S.; Nolan, S. P. *Acc. Chem. Res.* **2008**, *41*, 349–358.
(25) Marion, N.; Nolan, S. P. *Acc. Chem. Res.* **2008**, *41*, 1440–1449.
(26) Würtz, S.; Glorius, F. *Acc. Chem. Res.* **2008**, *41*, 1523–1533.
(27) Jurkauskas, V.; Sadighi, J. P.; Buchwald, S. L. *Org. Lett.* **2003**, *5*, 2417–2420.
(28) Gómez, F. J.; Kamber, N. E.; Deschamps, N. M.; Cole, A. P.; Wender, P. A.; Waymouth, R. M. *Organometallics* **2007**, *26*, 4541–4545.
(29) Praetorius, J. M.; Crudden, C. M. *Dalton Trans.* **2008**, 4079–4094.
(30) Trnka, T. M.; Grubbs, R. H. *Acc. Chem. Res.* **2001**, *34*, 18–29.
(31) Fogg, D. E.; dos Santos, E. N. *Coord. Chem. Rev.* **2004**, *248*, 2365–2379.
(32) Camm, K. D.; Castro, N. M.; Liu, Y.; Czechura, P.; Snelgrove, J. L.; Fogg, D. E. *J. Am. Chem. Soc.* **2007**, *129*, 4168–4169.
(33) Drouin, S. D.; Zamanian, F.; Fogg, D. E. *Organometallics* **2001**, *20*, 5495–5497.
(34) Zanardi, A.; Mata, J. A.; Peris, E. *J. Am. Chem. Soc.* **2009**, *131*, 14531–14537.
(35) Zanardi, A.; Corberán, R.; Mata, J. A.; Peris, E. *Organometallics* **2008**, *27*, 3570–3576.
(36) Burling, S.; Paine, B. M.; Nama, D.; Brown, V. S.; Mahon, M. F.; Prior, T. J.; Pregosin, P. S.; Whittlesey, M. K.; Williams, J. M. J. *J. Am. Chem. Soc.* **2007**, *129*, 1987–1995.
(37) Lillo, V.; Mata, J. A.; Segarra, A. M.; Peris, E.; Fernandez, E. *Chem. Commun.* **2007**, 2184–2186.
(38) Welle, A.; Díez-González, S.; Tinant, B.; Nolan, S. P.; Riant, O. *Org. Lett.* **2006**, *8*, 6059–6062.
(39) Sierra, M. A.; Amo, J. C. d.; Mancheño, M. J.; Gómez-Gallego, M.; Torres, M. R. *Chem. Commun.* **2002**, 1842–1843.
(40) Goldman, A. S.; Roy, A. H.; Huang, Z.; Ahuja, R.; Schinski, W.; Brookhart, M. *Science* **2006**, *312*, 257–261.
(41) Northrup, A. B.; MacMillan, D. W. C. *Science* **2004**, *305*, 1752–1755.
(42) Weatherhead, G. S.; Cortez, G. A.; Schrock, R. R.; Hoveyda, A. H. *Proc. Natl. Acad. Sci. U.S.A.* **2004**, *101*, 5805–5809.
(43) Periana, R. A.; Mironov, O.; Taube, D.; Bhalla, G.; Jones, C. *Science* **2003**, *301*, 814–818.
(44) Oishi, S.; Yoshimoto, J.; Saito, S. *J. Am. Chem. Soc.* **2009**, *131*, 8748–8749.
(45) Zhong, S.; Fu, Z.; Tan, Y.; Xie, Q.; Xie, F.; Zhou, X.; Ye, Z.; Peng, G.; Yin, D. *Adv. Synth. Catal.* **2008**, *350*, 802–806.
(46) Niu, F.; Zhai, J.; Jiang, L.; Song, W.-G. *Chem. Commun.* **2009**, 4738–4740.
(47) Samachetty, H. D.; Lemieux, V.; Brand, N. R. *Polyhedron* **2008**, *64*, 8292–8300.
(48) Liu, G.; He, H.; Wang, J. *Adv. Synth. Catal.* **2009**, *351*, 1610–1620.
(49) Ringenberg, M. R.; Kokatam, S. L.; Heiden, Z. M.; Rauchfuss, T. B. *J. Am. Chem. Soc.* **2008**, *130*, 788–789.
(50) Fujiwara, M.; Terashima, S.; Endo, Y.; Shiokawa, K.; Ohue, H. *Chem. Commun.* **2006**, 4635–4637.
(51) Gregson, C. K. A.; Gibson, V. C.; Long, N. J.; Marshall, E. L.; Oxford, P. J.; White, A. J. P. *J. Am. Chem. Soc.* **2006**, *128*, 7410–7411.
(52) Süssner, M.; Plenio, H. *Angew. Chem., Int. Ed.* **2005**, *44*, 6885–6888.
(53) Allgeier, A. M.; Mirkin, C. A. *Angew. Chem., Int. Ed.* **1998**, *37*, 894–908.
(54) Slone, C. S.; Mirkin, C. A.; Yap, G. P. A.; Guzei, I. A.; Rheingold, A. L. *J. Am. Chem. Soc.* **1997**, *119*, 10743–10753.
(55) Hembre, R. T.; McQueen, J. S.; Day, V. W. *J. Am. Chem. Soc.* **1996**, *118*, 798–803.
(56) Lorkovic, I. M.; Wrighton, M. S.; Davis, W. M. *J. Am. Chem. Soc.* **1994**, *116*, 6220–6228.
(57) Lorkovic, I. M.; Duff, R. R., Jr.; Wrighton, M. S. *J. Am. Chem. Soc.* **1995**, *117*, 3617–3618.

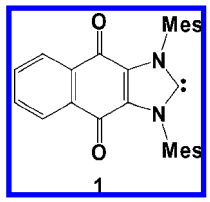

1

Figure 2. 1,3-Dimesitylnapthoquinimidazolylidene (**1**), an NHC comprising a redox-active naphthoquinone moiety.

Given the utility of NHC-supported Group 10 catalysts for a broad range of organic transformations,[17,25,26,58−62] and the relative ease of incorporating redox-active functionalities within NHC frameworks,[63−67] we envisioned that a complex comprising both attributes could enable RSC. We thus sought to prepare a family of Group 10 complexes bearing redox-active NHCs, to study their spectroscopic, structural, and electrochemical features, and to explore their potential for catalyzing organic transformations. We previously communicated naphthoquinimidazolylidene **1** and showed that its electron-donating character could be modified via reduction of the quinone to a semiquinone radical anion (Figure 2).[68] Building on these preliminary findings, we believed that Group 10 complexes supported by this redox-active NHC could exhibit interesting electronic properties in addition to catalyzing cross-coupling reactions and enabling redox-switchable control over these reactions. The results of our comprehensive studies are presented herein.

Experimental Section

Materials and Methods. Nickel(II), palladium(II), and platinum(II) chloride were purchased from Pressure Chemicals. 1,3-Dimesitylformamidine,[69] $[NiCl_2(PPh_3)_2]$,[70] *trans*-$[PdCl_2(PhCN)_2]$,[71] and *trans*-$[PtCl_2(PhCN)_2]$[72] were prepared as previously described. All other materials and solvents were of reagent quality and used as received. ^1H and $^{13}C\{^1H\}$ NMR spectra were recorded using a Varian 300, 400, 500, or 600 MHz spectrometer. Chemical shifts δ (in ppm) are referenced to tetramethylsilane using the residual solvent as an internal standard. For ^1H NMR: $CDCl_3$, 7.24 ppm. For ^{13}C NMR: $CDCl_3$, 77.0 ppm. Coupling constants (J) are expressed in hertz. High-resolution mass spectra (HRMS) were obtained with a VG analytical ZAB2-E instrument (ESI or CI). Elemental analyses were performed by Midwest Microlabs (Indianapolis, IN). Gas chromatography (GC) was performed on an Agilent 6850 gas chromatograph (HP-1 column, L = 30 m, I.D. = 0.32 mm, linear gradient: 50–300 °C, 20 °C min^{-1}). All syntheses were performed under ambient conditions unless specified otherwise.

Electrochemistry. Electrochemical experiments were conducted on CH Instruments Electrochemical Workstations (series 660D) using a gastight, three-electrode cell under an atmosphere of dry nitrogen. The cell was equipped with gold working and tungsten counter electrodes, as well as a silver wire quasi-reference electrode. Unless specified otherwise, measurements were performed using 1.0 mM solutions of analyte in dry CH_2Cl_2 with 0.1 M [tetra-*n*-butylammonium][PF_6] as the electrolyte and decamethylferrocene (Fc*) as the internal standard. Differential pulse voltammetry measurements were performed using 50 mV pulse amplitudes and 2 mV data intervals. Chronoamperometry experiments were performed using a 25 μm diameter gold ultramicroelectrode as the working electrode, enabling independent determination of D_0 and n by plotting $i(t)/i_{ss}$ vs $t^{-1/2}$ and using the Cottrell equation.[73] Data deconvolution and fitting were performed using the Origin 8.0 software package. All potentials listed herein were determined by cyclic voltammetry at 100 mV s^{-1} scan rates and referenced to a saturated calomel electrode (SCE) by shifting $(Fc^*)^{0/+}$ to −0.057 V (CH_2Cl_2).[74]

General Spectroscopic Considerations. UV−visible absorption spectra were recorded on a Perkin-Elmer Lambda 35 spectrometer. All room-temperature measurements were made using matched 6Q Spectrosil quartz cuvettes (Starna) with 1 cm path lengths and 3.0 mL of sample solution. Absorption spectra were acquired in CH_2Cl_2 under ambient conditions for all complexes. Extinction coefficients (ε) were determined from Beer's law measurements using 10, 20, 30, and 40 μM concentrations of the analyte.

1,3-Dimesitylnapthoquinimidazolium Chloride [1H][Cl]. 2,3-Dichloronaphthoquinone (1.13 g, 4.98 mmol) and *N*,*N*′-dimesitylformamidine (2.80 g, 9.99 mmol) were dissolved with 25 mL of CH_3CN in a heavy-walled flask equipped with a stir bar. The flask was sealed, and the reaction was then heated to 110 °C. After 48 h, the reaction was allowed to cool to room temperature, whereupon $NaHCO_3$ (420 mg, 5.00 mmol) was added, and the reaction mixture was then heated to 60 °C. After 16 h, the vessel was allowed to cool to room temperature, and then the reaction mixture was filtered through Celite to remove NaCl and the filtrate solvent was removed under reduced pressure. The resulting residue was then taken up in a minimal amount of CH_2Cl_2, filtered through a 0.2 μm PTFE filter, and added to 20 volume equivalents of Et_2O. The precipitated solids were collected via filtration, washed successively with THF and Et_2O, and then dried to afford 2.32 g (4.93 mmol, 99% yield) of the desired product as a yellow powder. Spectral data were consistent with literature values.[68]

[AgCl(1)] (2). To a solution of [**1**H][Cl] (1.18 mg, 2.51 mmol) in CH_2Cl_2 (15 mL) was added 3 Å molecular sieves, followed by Ag_2O (290 mg, 1.25 mmol) in CH_2Cl_2 (10 mL), and the resulting reaction mixture was allowed to stir at room temperature. After 16 h, the reaction mixture was filtered through a 0.2 μm PTFE filter, the filtrate solvent was removed under reduced pressure and the resulting solid was washed successively with THF and Et_2O, and then dried to afford 1.42 g (2.46 mmol, 98% yield) of the desired product as a bright yellow solid. Spectral data were consistent with literature values.[68]

General Procedure for the Synthesis of *trans*-[MCl_2(1)$_2$] Complexes. To a suspension of **2** (116 mg, 0.201 mmol) in toluene (3 mL) was added $[NiCl_2(PPh_3)_2]$ (65 mg, 99 μmol for **3a**), *trans*-$[PdCl_2(PhCN)_2]$ (40 mg, 0.10 mmol for **3b**), or *trans*-$[PtCl_2(PhCN)_2]$ (49 mg, 0.10 mmol for **3c**) in toluene (3 mL), and the resulting mixture was then heated to 110 °C. After 16 h, the mixture was

(58) Douthwaite, R. E. *Coord. Chem. Rev.* **2007**, *251*, 702–717.
(59) Christmann, U.; Vilar, R. *Angew. Chem., Int. Ed.* **2005**, *44*, 366–374.
(60) Miura, M. *Angew. Chem., Int. Ed.* **2004**, *43*, 2201–2203.
(61) Herrmann, W. A.; Ofele, K.; Preysing, D. v.; Schneider, S. K. *J. Organomet. Chem.* **2003**, *687*, 229–248.
(62) Culkin, D. A.; Hartwig, J. F. *Acc. Chem. Res.* **2003**, *36*, 234–245.
(63) Varnado, C. D., Jr.; Lynch, V. M.; Bielawski, C. W. *Dalton Trans.* **2009**, *7253*, 7261.
(64) Rosen, E. R.; Varnado, C. D.; Tennyson, A. G.; Khramov, D. M.; Kamplain, J. W.; Sung, D. H.; Creswell, P. J.; Lynch, V. M.; Bielawski, C. W. *Organometallics* **2009**, *28*, 6695–6706.
(65) Bildstein, B.; Malaun, M.; Kopacka, H.; Wurst, K.; Mitterböck, M.; Ongania, K.-H.; Opromolla, G.; Zanello, P. *Organometallics* **1999**, *18*, 4325–4336.
(66) Bildstein, B.; Malaun, M.; Kopacka, H.; Ongania, K.-H.; Wurst, K. *J. Organomet. Chem.* **1999**, *572*, 177–187.
(67) Bildstein, B.; Malaun, M.; Kopacka, H.; Ongania, K.-H.; Wurst, K. *J. Organomet. Chem.* **1998**, *552*, 45–61.
(68) Sanderson, M. D.; Kamplain, J. W.; Bielawski, C. W. *J. Am. Chem. Soc.* **2006**, *128*, 16514–16515.
(69) Kuhn, K. M.; Grubbs, R. H. *Org. Lett.* **2008**, *10*, 2075–2077.
(70) Quasdorf, K. W.; Tian, X.; Garg, N. K. *J. Am. Chem. Soc.* **2008**, *130*, 14422–14423.
(71) Braunstein, P.; Bender, R.; Jud, J. *Inorg. Synth.* **1989**, *26*, 341–350.
(72) Cardinaels, T.; Ramaekers, J.; Nockemann, P.; Driesen, K.; Hecke, K. V.; Meervelt, L. V.; Lei, S.; Feyter, S. D.; Guillon, D.; Donnio, B.; Binnemans, K. *Chem. Mater.* **2008**, *20*, 1278–1291.
(73) Bard, A. J.; Faulkner, L. R. *Electrochemical Methods: Fundamentals and Applications*, 2nd ed.; John Wiley & Sons, Inc.: Hoboken, NJ, 2001.
(74) Noviandri, I.; Brown, K. N.; Fleming, D. S.; Gulyas, P. T.; Lay, P. A.; Masters, A. F.; Phillips, L. *J. Phys. Chem. B* **1999**, *103*, 6713–6722.

Scheme 1. Improved Syntheses for [**1**H][Cl] and **2**[a]

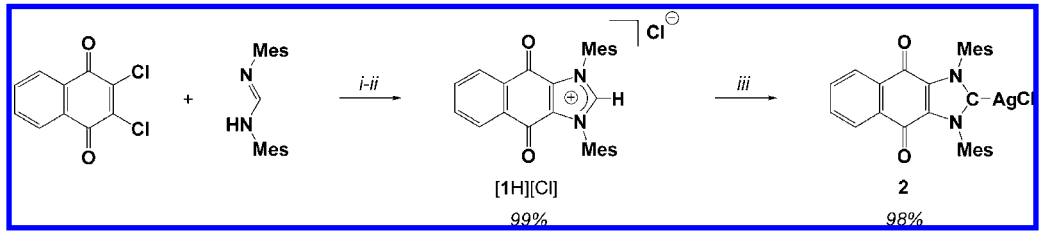

[a] Reagents and conditions: (*i*) 2 equiv of *N*,*N*′-dimesitylformamidine, CH_3CN, 110 °C; (*ii*) 1 equiv of $NaHCO_3$, 60 °C, 16 h; (*iii*) 0.5 equiv of Ag_2O, 3 Å molecular sieves, CH_2Cl_2, 16 h.

allowed to cool to room temperature and then filtered through a 0.2 μm PTFE filter with the aid of THF, and the filtrate solvent was removed under reduced pressure. The resulting residue was taken up in minimum CH_2Cl_2 and added to 10 volume equivalents of hexanes to induce precipitation. A total of three precipitations were performed (to remove residual PPh_3 or PhCN), and the resulting solids were collected via filtration, washed with Et_2O, and then dried to afford the desired complex. Isolated yields and spectroscopic data are reported below.

***trans*-[$NiCl_2$(**1**)$_2$] (3a).** Obtained as a dark orange powder (98 mg, 98 μmol, 99% yield). ^{1}H NMR (300 MHz, $CDCl_3$): δ 7.94 (q, J = 3.1, 4H), 7.64 (q, J = 3.1, 4H), 7.08 (s, 8H), 2.63 (s, 12H), 1.90 (s, 24H). ^{13}C NMR (75 MHz, $CDCl_3$): δ 181.2, 173.7, 138.2, 135.7, 134.1, 133.6, 132.3, 131.7, 129.5, 126.8, 21.6, 18.9. HRMS calcd for $C_{58}H_{52}ClN_4O_4Ni$ [M^+]: 998.2674. Found: 998.2689. Anal. Calcd for $C_{62}H_{62}Cl_2N_4O_5Ni$ [**3a**·Et_2O]: C, 69.41; H, 5.83; N, 5.22. Found: C, 69.52; H, 5.75; N, 5.49.

***trans*-[$PdCl_2$(**1**)$_2$] (3b).** Obtained as a bright yellow powder (102 mg, 97.5 μmol, 98% yield). ^{1}H NMR (300 MHz, $CDCl_3$): δ 7.97 (q, J = 2.8, 4H), 7.66 (q, J = 2.8, 4H), 6.99 (s, 8H), 2.55 (s, 12H), 1.90 (s, 24H). ^{13}C NMR (75 MHz, $CDCl_3$): δ 183.0, 173.9, 138.3, 136.3, 135.4, 134.3, 133.2, 132.4, 131.8, 129.3, 127.0, 21.5, 18.8. HRMS calcd for $C_{58}H_{52}ClN_4O_4Pd$ [$(M - Cl)^+$]: 1009.27064. Found: 1009.27071. Anal. Calcd for $C_{58}H_{52}Cl_2N_4O_4Pd$: C, 66.57; H, 5.01; N, 5.35. Found: C, 66.67; H, 5.07; N, 5.22.

***trans*-[$PtCl_2$(**1**)$_2$] (3c).** Obtained as a yellow-orange powder (112 mg, 98.8 μmol, 99% yield). ^{1}H NMR (300 MHz, $CDCl_3$): δ 7.97 (q, J = 2.9, 4H), 7.67 (q, J = 3.0, 4H), 6.97 (s, 8H), 2.54 (s, 12H), 1.88 (s, 24H). ^{13}C NMR (75 MHz, $CDCl_3$): δ 178.1, 174.0, 138.1, 135.3, 134.3, 133.3, 132.2, 131.8, 129.2, 126.9, 21.5, 18.7. HRMS calcd for $C_{58}H_{52}Cl_2N_4O_4Pt$ [M^+]: 1133.30079. Found: 1133.30315. Anal. Calcd for $C_{58}H_{52}Cl_2N_4O_4Pt$: C, 61.37; H, 4.62; N, 4.94. Found: C, 61.21; H, 4.95; N, 4.65.

General Procedure for Kumada Coupling Reactions. Bromoarene (0.10 mmol), PhMgCl (79 μL, 25 wt % in THF, 0.15 mmol), and **3** (5.0 μmol) were each dissolved with 1.0 mL of THF in separate vials. To the vigorously stirred bromoarene solution was added the solution of PhMgCl followed by the solution of **3**, accompanied by mesitylene (0.10 mmol) as an internal GC standard, and the reaction was allowed to stir at room temperature. After 24 h, an aliquot (0.1 mL) was removed and quenched via addition to wet hexanes (1.0 mL), filtered through a 0.2 μm PTFE filter, and analyzed by GC.

Controlling Kumada Coupling Activity of 3a via Redox Switching. Bromoarene (0.30 mmol), PhMgCl (237 μL, 25 wt % in THF, 0.45 mmol), and **3** (15 μmol) were each dissolved with 3.0 mL of THF in separate vials. To the bromoarene solution were added the solutions of PhMgCl and **3a**, followed by mesitylene (0.30 mmol) as an internal GC standard, and the reaction was allowed to stir at room temperature. Aliquots (0.1 mL each) were then withdrawn at 30 min intervals for 2 h, whereupon $CoCp_2$ (30 μmol, Cp = cyclopentadienyl) was added. As before, aliquots (0.1 mL each) were then withdrawn at 30 min intervals for 2 h, whereupon [Fc][BF_4] (30 μmol, Fc = $FeCp_2$) was added. Aliquots (0.1 mL each) were then withdrawn at 30 min intervals for 2 h and analyzed.

Table 1. Summary of Physical and Spectroscopic Data for [**1**H][Cl], **2**, and **3**[a]

	yield (%)	δC_{NHC} (ppm)	$\delta C_{C=O}$ (ppm)	ν_{CO} (cm^{-1})
[**1**H][Cl]	99	181.1	173.7	1685
2	98	150.5	164.9	1681
3a	99	181.2	173.7	1680
3b	98	183.0	173.9	1680
3c	99	178.1	174.0	1680

[a] ^{13}C NMR and IR measurements performed in $CDCl_3$ and KBr matrices, respectively.

Scheme 2. Syntheses of **3a**–**c**

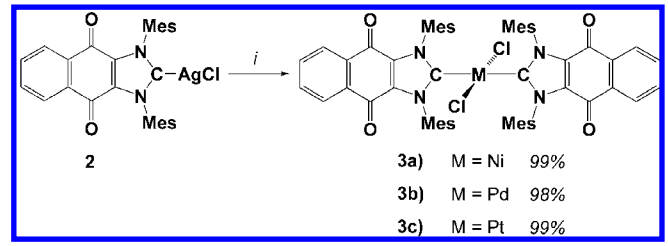

Results and Discussion

Synthesis and Characterization. Both [**1**H][Cl] and **2** have been previously reported, albeit with suboptimal yields (74% and 75%, respectively).[68] In the original procedure for [**1**H][Cl], Na_2SO_4 was employed to drive the reaction. Recently, we found that performing the synthesis with an additional equivalent of *N*,*N*′-dimesitylformamidine as sacrificial base afforded a 1:1 mixture of [**1**H][Cl] and *N*,*N*′-dimesitylformamidinium chloride in quantitative yield, as judged by ^{1}H NMR spectroscopy. Unfortunately, these compounds could not be separated due to their nearly identical solubilities. To overcome this limitation, we utilized the greater acidity of the formamidinium vs [**1**H][Cl]: treatment of the reaction mixture with 1 equiv of $NaHCO_3$ selectively neutralized the formamidinium byproduct, which was then extracted upon washing with Et_2O. Using this modified synthesis, the isolated yield of [**1**H][Cl] was improved from 74% to 99% (see Scheme 1 and Table 1). Similarly, by treating [**1**H][Cl] with 0.5 equiv Ag_2O for 16 h in CH_2Cl_2 at room temperature, as opposed to 90 °C for 12 h as in our original procedure, the yield of **2** was enhanced from 75% to 98%.

All attempts to coordinate free **1** to various nickel(II), palladium(II), or platinum(II) halide sources resulted in decomposition of the NHC, as determined by NMR spectroscopy. Similarly, reaction of **2** with 0.5 equiv of [$NiCl_2(PPh_3)_2$], *trans*-[$PdCl_2(PhCN)_2$], or *trans*-[$PtCl_2(PhCN)_2$] in THF, CH_2Cl_2, or CH_3CN afforded a complex mixture of products including a

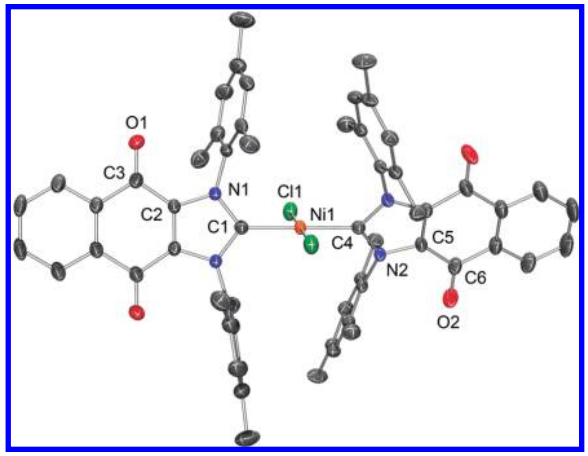

Figure 3. ORTEP diagram rendered using the POV-Ray engine, shown with 50% probability thermal ellipsoids and selected atom labels for **3a**. Hydrogen atoms and solvent molecules have been omitted for clarity. Selected distances (Å) and angles (°): Ni1−Cl1, 2.1701(10); Ni1−C1, 1.910(4); Ni1−C4, 1.910(4); N1−C1, 1.368(3); N1−C2, 1.384(4); N2−C4, 1.372(3); N2−C5, 1.383(4); O1−C3, 1.216(4); O2−C6, 1.221(4); C2−C3, 1.471(4); C5−C6, 1.468(4); N1−C1−N1′, 104.8(3); N2−C4−N2′, 104.5(3); N1−C1−Ni1−Cl1, 111.68(13); N2−C4−Ni1−Cl1, 108.60(13).

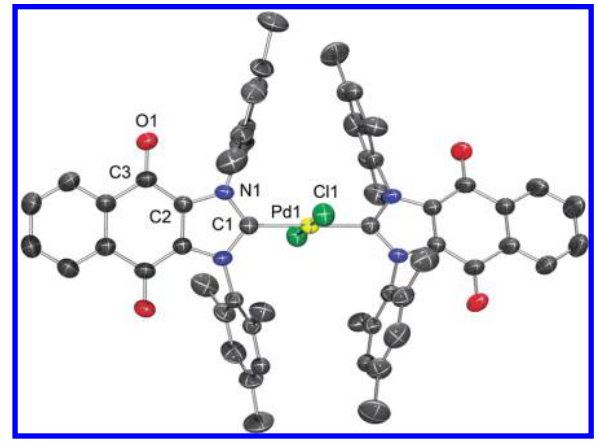

Figure 4. ORTEP diagram rendered using the POV-Ray engine, shown with 50% probability thermal ellipsoids and selected atom labels for **3b**. Hydrogen atoms have been omitted for clarity. Selected distances (Å) and angles (°): Pd1−Cl1, 2.3029(16); Pd1−C1, 2.021(6); N1−C1, 1.362(6); N1−C2, 1.390(6); O1−C3, 1.232(6); C2−C3, 1.444(7); N1−C1−N1′, 105.1(5); N1−C1−Ni1−Cl1, 73.0(2).

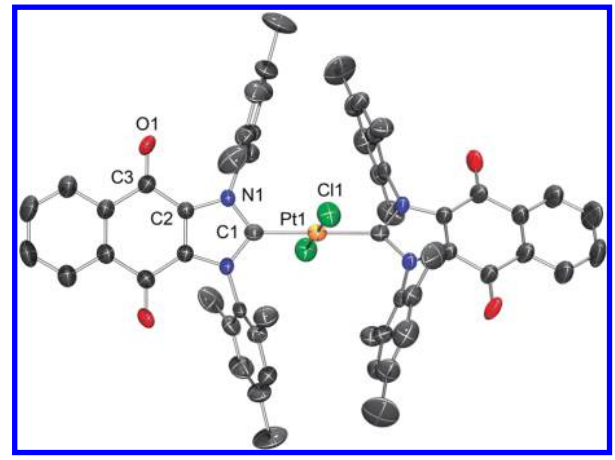

Figure 5. ORTEP diagram rendered using the POV-Ray engine, shown with 50% probability thermal ellipsoids and selected atom labels for **3c**. Hydrogen atoms have been omitted for clarity. Selected distances (Å) and angles (°): Pt1−Cl1, 2.309(2); Pt1−C1, 2.014(7); N1−C1, 1.373(5); N1−C2, 1.377(6); O1−C3, 1.226(7); C2−C3, 1.470(7); N1−C1−N1′, 104.3(5); N1−C1−Pt1−Cl1, 70.3(2).

significant quantity of unreacted starting material. However, transmetalation was successfully effected by performing the reaction in toluene at 110 °C for 16 h, producing *trans*-$[MCl_2(\mathbf{1})_2]$ in near-quantitative yields (**3a**, M = Ni, 99%; **3b**, M = Pd, 98%; **3c**, M = Pt, 99%; see Scheme 2 and Table 1). On the basis of these results, we surmise that the formation of **3** depended strongly on the kinetics of the transmetalation reaction, wherein the driving force was the release and precipitation of AgCl. In toluene, this occurred immediately and quantitatively, whereas more polar solvents may allow the formation of charged Ag_xCl_y species that are capable of re-forming [**1**H][Cl] or facilitate undesired reactivity. Overall, complexes **3a**−**c** were obtained in near-quantitative yields (95% to 96%) after three steps from commercially available starting materials.

The ^{13}C NMR chemical shifts of the NHC and quinone carbons for **3a**−**c** all fell within a narrow range (δC_{NHC} = 178.0−183.0 ppm and $\delta C_{C=O}$ = 173.7−174.0 ppm vs $CDCl_3$; Table 1), consistent with their congeneric nature. The chemical shifts for the carbene carbons in **3a**−**c** were higher than the values observed in other *trans*-$[MCl_2(NHC)_2]$ Group 10 complexes (160.2−174.6 ppm), reflecting the diminished electron density at the carbene nucleus in **1** vs those in classical imidazolylidene- or benzimidazolylidene-based NHCs.[75−84] Subsequent analysis of the quinone carbonyl stretching frequencies revealed indistinguishable energies (ν_{CO} = 1680 cm^{-1} in KBr), suggesting that the electron density within the naphthoquinone framework did not vary significantly whether **1** was bound to a first-, second-, or third-row transition metal.

Single crystals of **3a**−**c** suitable for X-ray diffraction were grown from saturated $CHCl_3$ solutions upon vapor diffusion of pentane. Crystallographic analysis revealed homologous structures for **3a**−**c** and confirmed their assignment as *trans*-$[MCl_2(\mathbf{1})_2]$ complexes (Figures 3−5). Although the Ni−C distance measured in **3a** (1.910(4) Å, see Table 2) occurred within the range of values observed with other *trans*-$[NiCl_2(NHC)_2]$ complexes (1.909−1.933 Å), its relatively short distance presumably reflects the greater π-acidity[68] of **1** compared to typical imidazolylidene-type NHCs.[80,83,85,86] Similarly, the Ni−Cl distance and N−C−N angles measured in **3a**

(75) Fu, C.-F.; Lee, C.-C.; Liu, Y.-H.; Peng, S.-M.; Warsink, S.; Elsevier, C. J.; Chen, J.-T.; Liu, S.-T. *Inorg. Chem.* **2010**, *49*, 3011–3018.
(76) Fahlbusch, T.; Frank, M.; Maas, G.; Schatz, J. *Organometallics* **2009**, *28*, 6183–6193.
(77) Ray, L.; Barman, S.; Shaikh, M. M.; Ghosh, P. *Chem.—Eur. J.* **2008**, *14*, 6646–6655.
(78) Ray, S.; Mohan, R.; Singh, J. K.; Samantaray, M. K.; Shaikh, M. M.; Panda, D.; Ghosh, P. *J. Am. Chem. Soc.* **2007**, *129*, 15042–15053.
(79) Ray, L.; Shaikh, M. M.; Ghosh, P. *Organometallics* **2007**, *26*, 958–964.
(80) Matsubara, K.; Ueno, K.; Shibata, Y. *Organometallics* **2006**, *25*, 3422–3427.
(81) Metallinos, C.; Barrett, F. B.; Chaytor, J. L.; Heska, M. E. A. *Org. Lett.* **2004**, *6*, 3641–3644.
(82) Liu, Q.-X.; Song, H.-B.; Xu, F.-B.; Li, Q.-S.; Zeng, X.-S.; Leng, X.-B.; Zhang, Z.-Z. *Polyhedron* **2003**, *22*, 1515–1521.
(83) MacKinnon, A. L.; Baird, M. C. *J. Organomet. Chem.* **2003**, *683*, 114–119.
(84) Tulloch, A. A. D.; Winston, S.; Danopoulos, A. A.; Eastham, G.; Hursthouse, M. B. *Dalton Trans.* **2003**, 699–708.
(85) Dible, B. R.; Sigman, M. S. *Inorg. Chem.* **2006**, *45*, 8430–8441.
(86) Herrmann, W. A.; Gerstberger, G.; Spiegler, M. *Organometallics* **1997**, *16*, 2209–2212.

Table 2. Structural Parameters for **3a**−**c**

	M−C (Å)	M−Cl (Å)	N−C−N (deg)
3a	1.910(4)	2.1701(10)	104.5(3),104.8(3)
3b	2.021(6)	2.3029(16)	105.1(5)
3c	2.014(7)	2.309(2)	104.3(5)

(2.1701(10) Å, 104.5(3)° and 104.8(3)°, respectively) were consistent with those measured in analogous NHC-supported complexes (Ni−Cl = 2.159−2.197 Å and N−C−N = 103.26−104.32°).[80,83,85,86]

As observed with **3a**, the M−C distances measured for the Pd and Pt congeners (2.021(6) and 2.014(7) Å for **3b** and **3c**, respectively; see Figures 4 and 5 as well as Table 2) agreed with those reported for other structurally characterized *trans*-$[MCl_2(NHC)_2]$ complexes (M = Pd, 1.977−2.081 Å; M = Pt, 2.005−2.044 Å).[78,79,82,84,87−95] In addition, complexes **3b** and **3c** exhibited M−Cl distances (M = Pd, 2.3029(16) Å; M = Pt, 2.3091(2) Å) and N−C−N angles (105.1(5)° and 104.3(5)°, respectively) that were consistent with those of other NHC-supported analogues (Pd, 2.298−2.359 Å and 101.28−106.93°; Pt, 2.313−2.636 Å and 101.73−105.81°). The nearly equivalent M−C and M−Cl distances measured in the Pd and Pt congeners arise from the lanthanide contraction in orbital radii that occurs upon going from a second- to a third-row transition metal.[96] Similarly, the M−C and M−Cl distances in **3b**,**c** were more than 0.1 Å longer than those in **3a**, reflecting the different ionic radii intrinsic to their metal centers (Ni, 0.63 Å; Pd, 0.78 Å; Pt, 0.74 Å).[96]

To complement the structural analysis of **3a**−**c**, we sought to examine their electronic features using electrochemical techniques. Previous studies by us[97] and others[98] have shown that the extent of metal−NHC interaction depends on their energy match (e.g., different behavior with iridium(I) vs iridium(III), iron(II) vs ruthenium(II), etc.) Therefore, we initially expected complexes **3a**−**c** to exhibit different electrochemical properties, given the variation in electronegativity of the metal centers (1.9 for Ni, 2.2 for Pd, and 2.3 for Pt).[96] However, the similarity among the ^{1}H NMR and IR spectroscopic features observed for **3a**−**c**, as well as their structural homology, suggested that the electrochemical behavior of these complexes might be highly conserved.

The cyclic voltammograms of **3a**−**c** in CH_2Cl_2 displayed broad, quasi-reversible reductions whose $E_{1/2}$ values were experimentally indistinguishable (**3a**, −0.75 V; **3b**, −0.72 V; **3c**, −0.73 V; see Figure 6 and Table 3).[99] Differential pulse voltammetry (DPV) followed by deconvolution revealed that these broad reductions comprised two underlying peaks, each of which was attributed to one-electron reductions of the quinone moieties in **1**. No significant variation in the $\Delta E_{1/2}$ values were observed (**3a**, 72 mV; **3b**, 76 mV; **3c**, 74 mV), indicating that the higher energy required for the second quinone reduction was most likely due to Coulombic effects, rather than any electronic communication between the two quinones across a bridging Group 10 metal.

Because the CVs of **3a**−**c** showed quasi-reversible quinone-based reductions, we next attempted bulk chemical reduction with the aim of isolating the reduced complexes. Addition of 2 equiv of $CoCp_2$ (Cp = cyclopentadienyl) to solutions of **3a**−**c** resulted in the formation of dark green suspensions.[100] Although these highly insoluble materials could not be characterized, subsequent treatment with 2 equiv of $[Fc][BF_4]$ (Fc = $FeCp_2$) afforded recovery of starting complexes, and mass-balance analysis indicated concomitant formation of 2 equiv of Fc and $[CoCp_2][BF_4]$. Attempts to exchange the $[CoCp_2]^+$ counterions with more soluble alternatives (e.g., Et_4N^+ or n-Bu_4N^+, introduced as their chloride salts), or to add $[CoCp_2]$ to solutions of **3a**−**c** already containing $[R_4N][Cl]$, resulted in the same dark green materials and quantitative recoveries of the cation-exchange reagents. Presumably, the inability to facilitate successful cation exchange reflected the insolubilities of the complexes formed via reduction of **3a**−**c** with $[CoCp_2]$. Such a complex, with the formula $[CoCp_2]_2[MCl_2(\mathbf{1}^-)_2]$, will be less soluble (↓) than the corresponding cation-exchange product $[CoCp_2][Cl]$ and thus will drive the equilibrium to the left (eq 1).

$$[CoCp_2]_2[MCl_2(\mathbf{1}^-)_2]\,(\downarrow) + 2R_4NCl \rightleftharpoons [R_4N]_2[MCl_2(\mathbf{1}^-)_2] + 2[CoCp_2][Cl] \quad (1)$$

To ascertain if the chemical and electrochemical reductions afforded the same complexes, we utilized UV−visible spectroelectrochemistry, wherein bulk electrolysis was performed at a sufficiently negative potential (E_{app} = −1.5 V) to reduce both NHC ligands in **3a**−**c**, and the optical difference spectra were recorded. In the neutral complexes **3a**−**c**, the primary features were observed at nearly identical energies (**3a**, 343 nm; **3b**, 342 nm; **3c**, 341 nm; see Figure 7A−C and Table 4), indicating that these $\pi \rightarrow \pi^*$ transitions were not sensitive to the identity of the Group 10 metal. These findings were in good agreement with the ^{1}H NMR and IR spectroscopic measurements described above, as well as the structural features revealed by crystallographic analysis. Upon reduction, the optical difference spectra showed sharp negative features at these wavelengths, corresponding to the consumption of the neutral complexes (Figure 7D−F). In addition, formation of the electrochemically reduced complexes afforded a broad, structured set of positive peaks above 600 nm (**3a**, 662 nm; **3b**, 641 nm; **3c**, 642 nm), corresponding to the source of the green color observed in the bulk chemical reduced species. Each reduced complex also displayed two well-defined positive peaks at higher energies (**3a**, 384 and 458 nm; **3b**, 382 and 455 nm; **3c**, 376 and 459 nm) that were invariant with the identities of the Group 10

(87) Fei, Z.; Zhao, D.; Pieraccini, D.; Ang, W. H.; Geldbach, T. J.; Scopelliti, R.; Chiappe, C.; Dyson, P. J. *Organometallics* **2007**, *26*, 1588–1598.
(88) Tewes, F.; Schlecker, A.; Harms, K.; Glorius, F. *J. Organomet. Chem.* **2007**, *692*, 4593–4602.
(89) Saravanakumar, S.; Oprea, A. I.; Kindermann, M. K.; Jones, P. G.; Heinicke, J. *Chem.—Eur. J.* **2006**, *12*, 3143–3154.
(90) Campeau, L.-C.; Thansandote, P.; Fagnou, K. *Org. Lett.* **2005**, *7*, 1857–1860.
(91) Frøseth, M.; Netland, K. A.; Törnroos, K. W.; Dhindsa, A.; Tilset, M. *Dalton Trans.* **2005**, 1664–1674.
(92) Hannig, F.; Kehr, G.; Fröhlich, R.; Erker, G. *J. Organomet. Chem.* **2005**, *690*, 5959–5972.
(93) Bonnet, L. G.; Douthwaite, R. E.; Hodgson, R.; Houghton, J.; Kariuki, B. M.; Simonovic, S. *Dalton Trans.* **2004**, 3528–3535.
(94) Lebel, H.; Janes, M. K.; Charette, A. B.; Nolan, S. P. *J. Am. Chem. Soc.* **2004**, *126*, 5046–5047.
(95) Newman, C. P.; Deeth, R. J.; Clarkson, G. J.; Rourke, J. P. *Organometallics* **2007**, *26*, 6225–6233.
(96) Cotton, F. A.; Wilkinson, G.; Murillo, C. A.; Bochmann, M. *Advanced Inorganic Chemistry*, 6th ed.; John Wiley & Sons, Inc.: New York, 1999.
(97) Tennyson, A. G.; Rosen, E. L.; Collins, M. S.; Lynch, V. M.; Bielawski, C. W. *Inorg. Chem.* **2009**, *48*, 6924–6933.
(98) Mercs, L.; Neels, A.; Albrecht, M. *Dalton Trans.* **2008**, 5570–5576.
(99) All potentials are reported relative to saturated calomel electrode (SCE).
(100) Similar results were obtained when using KC_8 as the reductant.

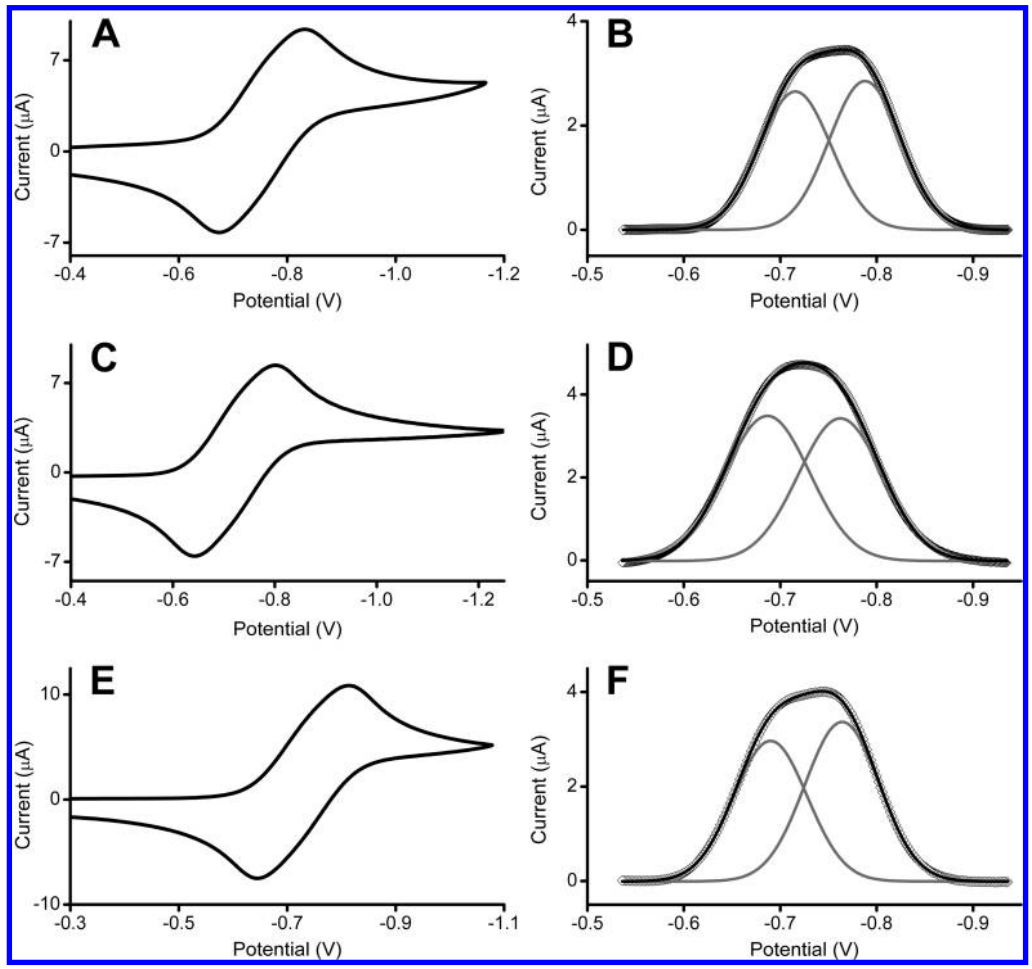

Figure 6. CV (100 mV s^{-1} scan rate) and DPV (50 mV pulse amplitude) of **3a** (A,B), **3b** (C,D), and **3c** (E,F) in CH_2Cl_2 containing 1.0 mM analyte and 0.1 M [nBu$_4$N][PF_6]. Overlaid on the DPV data for **3a**−**c** (B,D,F; open diamonds) are deconvoluted and fitted peaks represented by gray and black lines, respectively.

Table 3. Electrochemical Properties[a]

	$E_{1/2}$ (V)	$\Delta E_{1/2}$ (mV)
[**1**H][Cl]	−0.24	–
2	−0.49	–
3a	−0.75	72
3b	−0.72	76
3c	−0.73	74

[a] Measurements performed on 1.0 mM solutions of analyte in CH_2Cl_2 containing 0.1 M [Bu$_4$N][PF_6].

metals. The higher-energy peaks (<600 nm) were conserved among **3a**−**c** and had peak shapes similar to those in the neutral complexes, consistent with the assignment of these hypsochromic features as primarily ligand-centered $\pi \rightarrow \pi^*$ transitions. In contrast, the optical profile of the Ni complex was markedly distinct from those of its heavier congeners, with no difference between Pd and Pt (662 nm for **3a** vs 641 and 642 nm for **3b** and **3c**, respectively). On the basis of these results, we believe that these lower-energy transitions are metal-to-ligand charge transfer in nature and thus reflect the significantly different orbital energies for first-row vs second- and third-row transition metals.[101]

Redox-Switchable Catalysis: Controlling Kumada Cross-Coupling Activity. We aimed to build on the straightforward, near-quantitative syntheses of **3a**−**c** by demonstrating their practical utility in catalyzing cross-coupling reactions and, ultimately, their potential for achieving our goal of effecting RSC with Group 10 complexes supported by a redox-active NHC. To avoid the need for exogenous bases and any possible base-dependent reactivity, our initial investigations focused on Kumada cross-coupling reactions. Although the first NHC-supported Group 10 complex to catalyze a Kumada cross-coupling reaction was reported by Nolan in 1999, Pd^0 and elevated temperatures were needed for activity.[102] Since this study, improvements in complex stability, synthetic diversity, and catalyst activity have been realized.[25,26,59,61,103−111] Most notably, Wang recently reported a nickel complex bearing a tetradentate bis(NHC) that could catalyze Kumada cross-

(101) Kunkely, H.; Vogler, A. *J. Organomet. Chem.* **2003**, *684*, 113–116.
(102) Huang, J.; Nolan, S. P. *J. Am. Chem. Soc.* **1999**, *121*, 9889–9890.
(103) Glorius, F. *Top. Organomet. Chem.* **2007**, *21*, 1–20.
(104) Berding, J.; van Dijkman, T. F.; Lutz, M.; Spek, A. L.; Bouwman, E. *Dalton Trans.* **2009**, 6948–6955.
(105) Liu, A.; Zhang, X.; Chen, W. *Organometallics* **2009**, *28*, 4868–4871.
(106) Xi, Z.; Liu, B.; Chen, W. *J. Org. Chem.* **2008**, *73*, 3954–3957.
(107) Zhou, Y.; Xi, Z.; Chen, W.; Wang, D. *Organometallics* **2008**, *27*, 5911–5920.
(108) Organ, M. G.; Abdel-Hadi, M.; Avola, S.; Hadei, N.; Nasielski, J.; O'Brien, C. J.; Valente, C. *Chem.—Eur. J.* **2007**, *13*, 150–157.
(109) Schneider, S. K.; Rentzsch, C. F.; Krüger, A.; Raubenheimer, H. G.; Herrmann, W. A. *J. Mol. Catal. A: Chemical* **2007**, *265*, 50–58.
(110) Kremzow, D.; Seidel, G.; Lehmann, C. W.; Fürstner, A. *Chem.—Eur. J.* **2005**, *11*, 1833–1853.
(111) Frisch, A. C.; Rataboul, F.; Zapf, A.; Beller, M. *J. Organomet. Chem.* **2003**, *687*, 403–409.

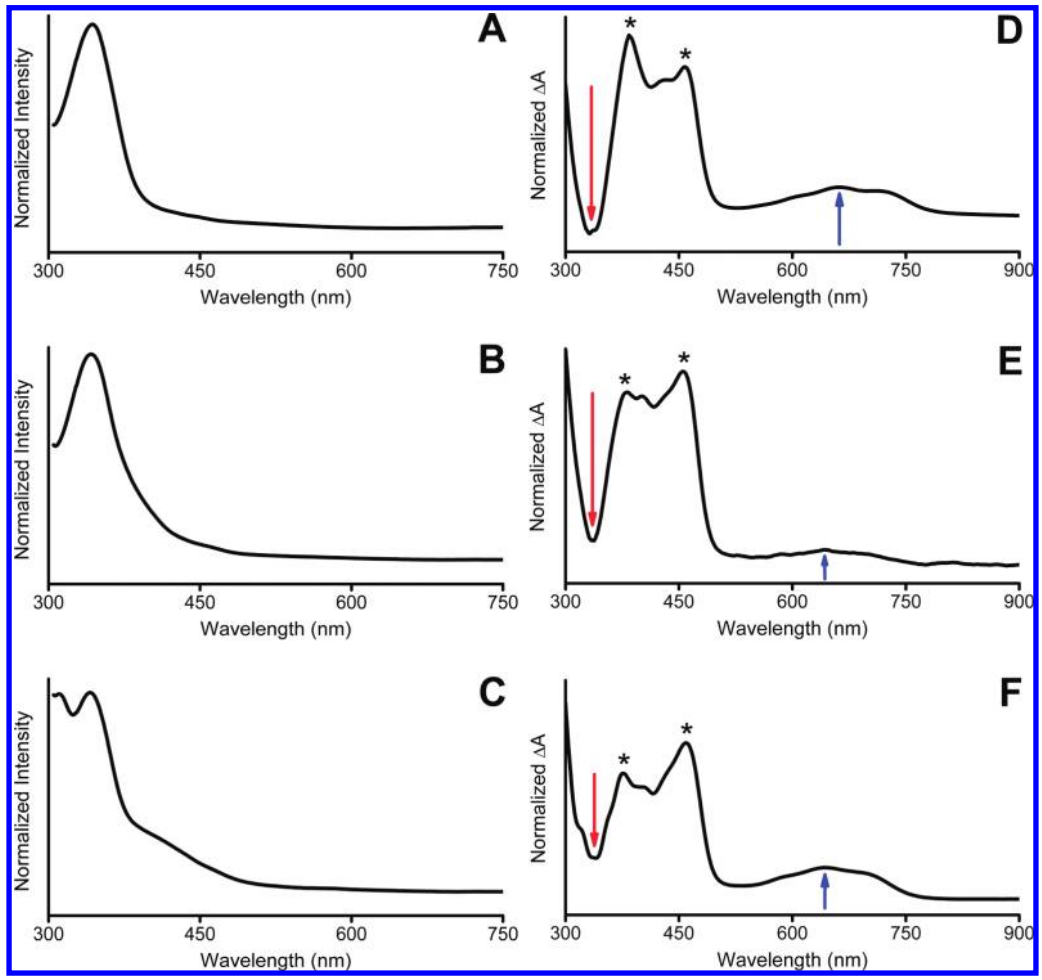

Figure 7. Normalized absorbance and spectroelectrochemical optical difference spectra, respectively, of **3a** (A,D), **3b** (B,E), and **3c** (C,F) in CH_2Cl_2. Red and blue arrows indicate consumption of the neutral complex and formation a long-wavelength peak indicative of the reduced complex, respectively. Conditions: 5 mM analyte, 0.1 M [nBu$_4$N][PF$_6$], $E_{app} = -1.5$ V.

Table 4. UV−Visible Properties of Neutral and Electrochemically Reduced Complexes

	λ (nm)		
		reduced[a]	
	neutral	$-\Delta A$	$+\Delta A$
3a	343	338	384, 458, 662
3b	342	338	382, 455, 641
3c	341	341	376, 459, 642

[a] Wavelengths corresponding to negative and positive features ($-\Delta A$ and $+\Delta A$) relative to neutral complex.

coupling reactions in less than 24 h at room temperature.[112] Unfortunately, the preparation of this catalyst requires multiple air-sensitive steps and a synthetically challenging azide-functionalized imidazolium salt precursor. Thus, an NHC-supported complex that combines ease of synthesis with high performance remains an important target for synthetic chemists.

As shown in Scheme 3, **3a** (5 mol %) was found to catalyze the coupling of *p*-bromoarene (**4a**−**c**; initial concentration = 30 mM) with PhMgCl (1.5 equiv) in THF, affording the corresponding 4-functionalized biphenyl (**5a**−**c**) in moderate to excellent yields after 24 h at room temperature, as determined by gas chromatography (67−93%).[113] A plausible explanation for the relatively high catalytic activity observed at room temperature is that the electron-withdrawing character of **1** stabilizes a nickel(0) oxidation state better than typical NHCs or phosphines, thus lowering the energy necessary for the reductive elimination step. Complex **3a** thus achieved our goal of effecting Kumada catalysis at room temperature on reasonable time scales, yet it was significantly more straightforward to synthesize than many analogous systems.

Scheme 3. Kumada Cross-Coupling Reactions Catalyzed by **3a**−**c**

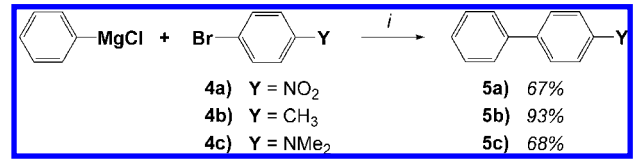

Considering that reduction of the quinone moieties in **3a**−**c** significantly altered the electronic topology at the metal centers therein, we envisioned that the catalytic activity of **3a** may be controlled via altering the redox state of the supporting NHC ligands. To test this hypothesis, the conversion of **4b** to **5b** catalyzed by **3a** in THF ([**4b**]$_0$ = 30 mM, 1.5 equiv PhMgCl, 5 mol % **3a**) was monitored by GC over 30 min intervals and

(112) Zhang, C.; Wang, Z.-X. *Organometallics* **2009**, *28*, 6507–6514.

(113) In contrast, no reactivity was observed with **3b** or **3c**, even under forcing conditions (reflux, >24 h). Analogous attempts to prepare **5a**−**c** using PhSnMe$_3$ under common Stille conditions were unsuccessful.

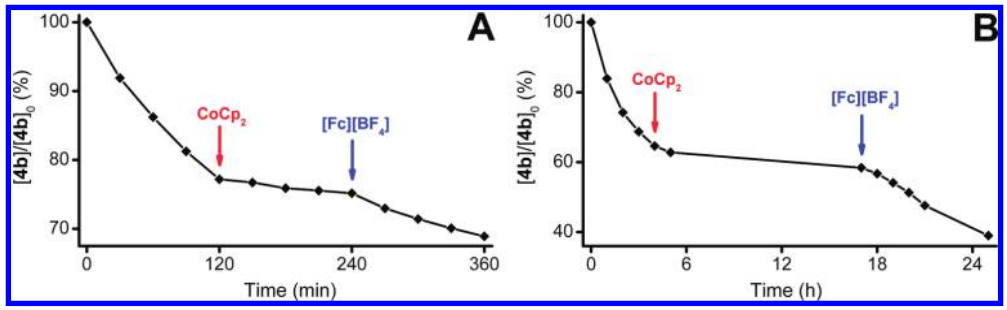

Figure 8. Percent conversion of **4b** to **5b** vs $[\mathbf{4b}]_0$ as catalyzed by **3a**. Conversions were determined by GC over two different time scales. An arrow with $CoCp_2$ or $[Fc][BF_4]$ indicates that 2 equiv of this reductant or oxidant (with respect to **3a**) was added to the reaction after the respective aliquot was removed.

found to proceed with a first-order rate constant (k_{obs}) of 4.7×10^{-5} s^{-1} (Figure 8A). After 2 h, $CoCp_2$ (2 equiv relative to Ni) was added to reduce **3a** and decreased the observed catalytic activity by an order of magnitude ($k_{obs} = 2.7 \times 10^{-6}$ s^{-1}). Two hours later, the introduction of $[Fc][BF_4]$ (2 equiv relative to Ni) afforded nearly a 5-fold restoration of catalytic activity ($k_{obs} = 1.2 \times 10^{-5}$ s^{-1}).[114] To probe the stability of the reduced state, we performed an analogous experiment where the catalyst was modulated to the reduced-activity state after 4 h via treatment with $CoCp_2$. Consistent with the aforementioned experiment, a decreased rate of **4b** consumption was observed (k_{obs} fell from 4.7×10^{-5} to 3.0×10^{-6} s^{-1}; Figure 8B). After allowing the reaction to remain in this state for 12 h, analysis by GC revealed that less than 5% of **4b** had been consumed, in marked contrast to nearly 40% in the first 4 h. Subsequent addition of $[Fc][BF_4]$ to the reduced catalyst afforded a restoration in Kumada activity to a level that was comparable with that of the previous experiment ($k_{obs} = 1.4 \times 10^{-5}$ vs 1.2×10^{-5} s^{-1}, respectively). Collectively, these results indicate that (1) the catalytic activity of **3a** in Kumada cross-coupling reactions can be decreased upon reduction, (2) the reduced catalyst is stable over extended periods of time, and (3) catalytic reactivation can be achieved via subsequent oxidation.[115,116]

To elucidate how the addition of $CoCp_2$ could modulate the catalytic activity of **3a**, we considered the mechanism and intermediates for a typical Kumada cross-coupling cycle. Initially, the Ni(II) center in **3a** is reduced by 2 equiv of PhMgCl to generate the catalytically active nickel(0) species $[Ni^0(\mathbf{1})_2]$, with concomitant formation of biphenyl and 2 equiv of $MgCl_2$ (Scheme 4). The reduced catalyst then undergoes oxidative addition with **4b** to afford $[Ni^{II}(Br)(p\text{-tol})(\mathbf{1})_2]$, which reacts with PhMgCl to produce $[Ni^{II}(Ph)(p\text{-tol})(\mathbf{1})_2]$. Subsequent reductive

Scheme 4. Proposed Mechanism for Arresting Catalysis of **3a** via Redox Changes

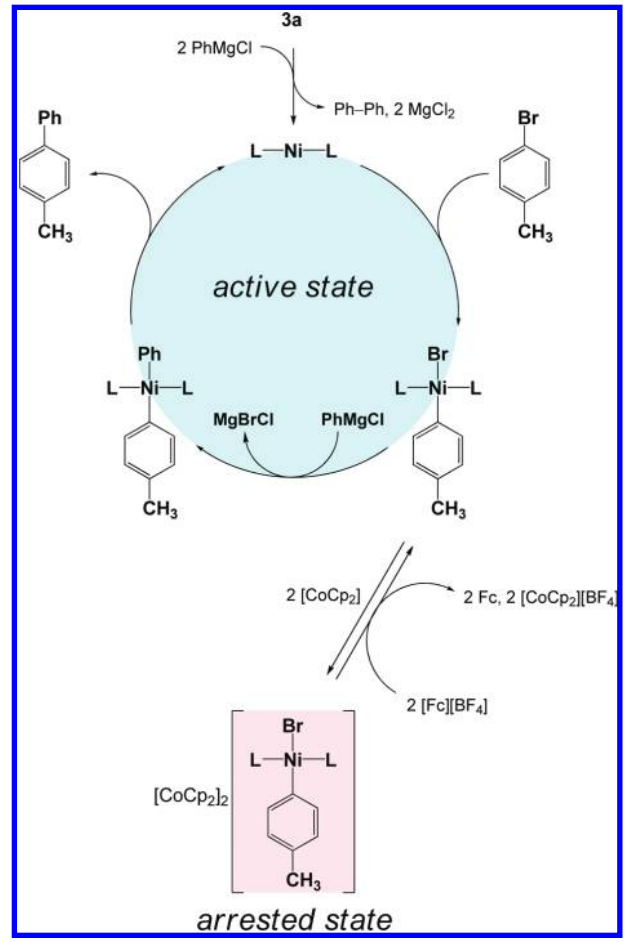

elimination then releases the desired cross-coupled product **5b**, regenerating $[Ni^0(\mathbf{1})_2]$ and enabling subsequent catalysis.

Of the nickel(II)-containing species in this cycle, we believe that $[Ni^{II}(Br)(p\text{-tol})(\mathbf{1})_2]$ would be the most easily reduced, given the greater σ-inductive effect of Br vs Ph. Supportive of this postulate, complexes of the form $[Ni^{II}(X)(Ar)(NHC)_2]$ have been previously described and shown to be thermally and air-stable.[117,118] Guided by this precedence and the redox chemistry of **3a** (vide supra), we surmise that the species formed upon treatment with $CoCp_2$ to a Kumada catalytic reaction is consistent with the formula $[CoCp_2]_2[Ni(Br)(p\text{-tol})(\mathbf{1})_2]$. To determine whether the addition of reductant shut down reactivity due to catalyst precipitation, we repeated the redox-switching experiment on a preparative scale (50 μmol) in **3a**. The cross-coupling was

(114) If the $[Fc][BF_4]$ were completely consumed via oxidation of PhMgCl, the amount of biphenyl observed by GC would double (increase 100%). However, the biphenyl peak in the corresponding gas chromatogram was found to increase by ~10% (some oxidation of PhMgCl does occur), indicating that most of the added oxidant reacts with the arrested catalyst. Empirically, this is borne out independently by the restoration in Kumada activity following the addition of $[Fc][BF_4]$.

(115) Although the oxidation of PhMgCl (E_0 = 0 V, see ref 116) can generate Ph•, this radical is still more oxidizing than **3a** ($E_{1/2}$ = −0.75 V vs. SCE), thus providing a strong *thermodynamic* driving force for the arrested catalyst to function as the ultimate reductant. Although Ph_2 can be formed from Ph•, the probability of this bimolecular collision is less than or equal to that with the arrested catalyst. Moreover, Ph• can oxidize the arrested catalyst via an outer-sphere electron transfer without necessitating a collisional reaction, thus providing the oxidation of the arrested catalyst with a significant *kinetic* driving force.

(116) Carloni, P.; Greci, L.; Stipa, P.; Eberson, L. *J. Org. Chem.* **1991**, *56*, 4733–4737.

allowed to proceed for 1 h, whereupon 2 equiv of $CoCp_2$ were added to halt the reaction, and 1 h later, the reaction was then filtered. No precipitate was recovered, even when using a 0.2 μm filter and the filtrate was homogeneous, suggesting that the catalytic cycle was not arrested via a change in solubility.[119]

Alternatively, we reasoned that the reduction of [Ni(Br)(*p*-tol)(**1**)$_2$] to [$CoCp_2$]$_2$[Ni(Br)(*p*-tol)(**1**)$_2$] could render catalyst turnover energetically inaccessible due to the electron-richness of the metal.[120] Although there is some ambiguity as to the formal oxidation state, whether this complex is [$CoCp_2$]$_2$[Ni^0(Br)(*p*-tol)(**1**)$_2$] or [$CoCp_2$]$_2$[Ni^{II}(Br)(*p*-tol)(**1**$^-$)$_2$], the metal center will be more electron rich following reduction. Consequently, transmetalation with PhMgCl will be more difficult, given that this step involves bond-formation between the metal and a negatively polarized carbon atom. Although [$CoCp_2$]$_2$[Ni(Ph)(*p*-tol)(**1**)$_2$] could be produced, reductive elimination of 4-methylbiphenyl would form [$CoCp_2$]$_2$[Ni(**1**)$_2$], comprising a [Ni^0(**1**$^-$)$_2$] core. Because the anionic form of **1** is more electron-donating than its neutral form, the reduction of a Ni(II) center bound to **1**$^-$ (an anionic NHC) will occur at higher energy than a Ni(II) center bound to **1** (neutral NHC), and thus at a slower rate. Since this complex is formally outside the catalytic cycle, it can no longer partake in the cross-coupling reaction, and thus it represents the catalyst in an "arrested" state.

Future efforts will be directed toward the challenging spectroscopic and structural elucidation of this arrested state, primarily to gain greater insight into the reduced catalyst and mechanism of redox switching thereof. Whereas the arrested state derived from **3a** does not participate in the Kumada coupling catalytic cycle, it is nonetheless an electron-rich complex that could potentially be competent for effecting orthogonal reactions. As such, we believe the results presented herein represent an important step toward a new, practical tandem catalysis strategy to achieve multiple, fundamentally distinct chemical transformations.

Conclusions

In sum, we have developed optimized syntheses of [**1**H][Cl] and **2**, thus enabling access to complexes **3a**−**c** in excellent overall yields from commercially available starting materials. Comprising a range of Group 10 metals, these complexes exhibit highly conserved ^{1}H NMR, IR, and UV/vis spectroscopic features, as well as structural homology. Electrochemical analysis of **3a**−**c** revealed two resolvable one-electron reductions, each corresponding to a quinone−semiquinone radical anion couple whose $E_{1/2}$ and $\Delta E_{1/2}$ values appeared to be insensitive to the identity of the bridging metal. Attempts to prepare and isolate the reduced complexes via bulk chemical reduction resulted in an intractable dark green solid, and UV/vis spectroelectrochemical measurements confirmed that this green color was consistent with bulk chemical reduction of **3a**−**c**.

Impressively, Ni complex **3a** was found to catalyze the Kumada cross-coupling between PhMgCl and bromoarenes **4a**−**c** at room temperature. Addition of $CoCp_2$ during the conversion of bromotoluene (**4b**) to 4-methylbiphenyl (**5b**) as catalyzed by **3a** resulted in a significant reduction in catalyst activity (from 4.7×10^{-5} to 2.7×10^{-6} s^{-1}), which was restored upon addition of [Fc][BF_4] ($k_{obs} = 1.2 \times 10^{-5}$ s^{-1}). We believe the diminished activity reflects the greater electron density at the metal center in [$CoCp_2$]$_2$[Ni(Br)(*p*-tol)(**1**)$_2$] vs [Ni(Br)(*p*-tol)(**1**)$_2$], causing the transmetalation and reductive elimination steps (necessary for turnover) to occur at a much slower rate. Collectively, these results expand upon the relatively few reported examples of reversibly redox-switchable catalysts and, to the best of our knowledge, represent the first example of a Kumada catalyst whose activity can be modulated via redox changes.

From a synthetic strategy viewpoint, this system represents a significant conceptual and practical advance toward the use of redox-switchable control as an effector of tandem or serial catalysis. Reduction of the catalyst precludes participation in the Kumada coupling cycle; however, the resulting reduced complex is both soluble and electron-rich, criteria which render it competent to perform other reactions. Given the wide range of organic transformation and polymerization reactions catalyzed by NHC-supported Group 10 complexes, some of which could be orthogonal/compatible with cross-coupling reactions, the ability to arrest catalytic activity via switching the redox state of **1** may enable new methodologies for the manipulation of catalytic reactions, particularly in tandem.

Acknowledgment. We thank S. Saravankumar for the initial efforts to obtain crystals of **3b**. We are grateful to the United States Army Research Office (W911NF-09-1-0446), the National Science Foundation (CHE-0645563), and the Robert A. Welch Foundation (F-1621) for financial support. The X-ray data for **3c** were collected using instrumentation purchased with funds provided by the National Science Foundation (CHE-0741973).

Supporting Information Available: Crystallographic data tables; ^{1}H and ^{13}C NMR spectra; CIF files. This material is available free of charge via the Internet at http://pubs.acs.org.

JA102686U

(117) Schaub, T.; Backes, M.; Radius, U. *J. Am. Chem. Soc.* **2006**, *128*, 15964–15965.
(118) McGuinness, D. S.; Cavell, K. J.; Skelton, B. W.; White, A. H. *Organometallics* **1999**, *18*, 1596–1605.
(119) This observation is consistent with the proposed mechanism: **3a** must be converted to the neutral, halide-free nickel(0) complex [Ni(**1**)$_2$] prior to entering the catalytic cycle. Moreover, none of the intermediate steps in this cycle feature two metal-bound halide ligands. Thus, the solubility of [$CoCp_2$]$_2$[Ni(Br)(*p*-tol)(**1**)$_2$] vs the insolubility of [$CoCp_2$]$_2$[$NiCl_2$(**1**)$_2$] reflects the solubilizing ability of the *p*-tol moiety in the former.
(120) Precipitating the filtrate into hexanes and washing with Et_2O to remove any **4b**, **5b**, PhMgCl, and magnesium salts afforded a THF-soluble, paramagnetic compound. Mass-balance analysis of the THF-soluble component corresponded to 82% of the theoretical yield of [$CoCp_2$]$_2$[Ni(Br)(*p*-tol)(**1**)$_2$].